Chemical Geology 577 (2021) 120285

Contents lists available at ScienceDirect

Chemical Geology

journal homepage: www.elsevier.com/locate/chemgeo

Invited Research Article

Insight into cyanobacterial preservation in shallow marine environments from experimental simulation of cyanobacteria-clay co-aggregation

Hongchang Liu [a,b], Peng Yuan [a,c,*], Dong Liu [a,c], Weiwei Zhang [b], Qian Tian [a,c], Hongling Bu [a,c], Yanfu Wei [a,c], Jinlan Xia [b], Yinchu Wang [d], Junming Zhou [a,c]

[a] CAS Key Laboratory of Mineralogy and Metallogeny/Guangdong Provincial Key Laboratory of Mineral Physics and Materials, Guangzhou Institute of Geochemistry, CAS Center for Excellence in Deep Earth Science, Chinese Academy of Sciences, Guangzhou 510640, China
[b] Key Lab of Biometallurgy of Ministry of Education of China, School of Minerals Processing and Bioengineering, Central South University, Changsha 410083, China
[c] University of Chinese Academy of Sciences, Beijing 100049, China
[d] Yantai Institute of Coastal Zone Research, Chinese Academy of Sciences, Yantai 264003, China

ARTICLE INFO

Editor: Dr. Hailiang Dong

Keywords:
Cyanobacteria-clay co-aggregates
Cyanobacterial preservation
Suspended clay minerals
Shallow marine environments

ABSTRACT

Clay minerals associated with microbial body and trace fossils in rocks deposited in shallow marine environments have importance in understanding microbial preservation. We show experimentally that the presence of suspended detrital clays in oceanic environments is a crucial control on the formation of co-aggregates between filamentous cyanobacteria and clay minerals and is thus important in the sedimentation and subsequent preservation of cyanobacteria. Strong cyanobacteria-clay co-aggregation occurs over short time periods (3–7 days) in the presence of 10 mg/L of suspended clay minerals (illite, kaolinite and montmorillonite), and the occurrence of co-aggregation is not affected by the type of clay minerals present. The cyanobacteria-clay co-aggregation shows a pronounced effect on preserving the biomass of cyanobacteria. The surface properties of clay minerals and cyanobacteria, specifically the electrostatic attraction between the oppositely charged surfaces of cyanobacteria and clay minerals, are the main drivers of cyanobacteria-clay co-aggregation. Chemical effects, such as the deprotonation of —COOH groups in active organic compounds secreted by cyanobacteria and therefore the release of H^+, result in local dissolution of clay and slight structure changes in the bulk of clay minerals. Compared with the suspended clay, dissolved ions (Si, Al or Fe ions) are of secondary importance in the formation of cyanobacteria-clay co-aggregates, although these ions further promote this process. Overall, the cyanobacteria-clay co-aggregation not only substantially affects the preservation of cyanobacteria, but also may have potentially important and profound impacts on related geochemical processes such as microbial dissolution of clay minerals and the biogeochemical Si cycle in marine environments.

1. Introduction

The occurrence of clay minerals on Earth's surface dates back to the aqueous alteration of chondrites (around 4.55 Ga) (Cuadros et al., 2013). Since then, the variety and volume of clays has increased and by the Proterozoic Eon they were an important component of marine sediments (Hu et al., 1998; Tosca et al., 2010). Over the past decades, clay minerals have been proposed as an important variable in the exceptional preservation of organisms lacking biomineralized parts, i.e., organic fossils. Many studies have shown clays directly associated with fossils in mudstones where clays make up a large fraction (~50%) of the rock, mostly focusing on iconic Burgess Shale-type (BST) preservation (e.g., Butterfield, 1990, 1995; Orr et al., 1998; Anderson et al., 2020a, 2020b). In BST preservation, organic material is retained and flattened parallel to bedding (Butterfield, 1995; Gaines, 2014). Anderson et al. (2018) found that the Cambrian mudstones in which BST fossils are preserved, as well as the fossils themselves, are enriched in specific clays. Experimental studies have shown these same clays are toxic to decay bacteria (McMahon et al., 2016), providing a mechanistic link between clays and exceptional preservation.

Clay minerals in sedimentary rocks that host the preservation of fossils may derive from detrital sources, or from authigenic or late stage

* Corresponding author at: CAS Key Laboratory of Mineralogy and Metallogeny/Guangdong Provincial Key Laboratory of Mineral Physics and Materials, Guangzhou Institute of Geochemistry, CAS Center for Excellence in Deep Earth Science, Chinese Academy of Sciences, Guangzhou 510640, China.
E-mail address: yuanpeng@gig.ac.cn (P. Yuan).

https://doi.org/10.1016/j.chemgeo.2021.120285
Received 22 November 2020; Received in revised form 22 April 2021; Accepted 26 April 2021
Available online 29 April 2021

(e.g., metamorphic) mineral growth (Wacey et al., 2014). Authigenic clay minerals have been speculated to contribute to microbial aggregation and sedimentation, and thus may have contributed to the preservation of wholly soft microbial organisms (Ferris et al., 1988; Brasier et al., 2011; Gauger et al., 2016). In the Precambrian ocean with the elevated concentrations of dissolved silica and metals (such as Fe and Al ions) (Fein et al., 2002; Gauger et al., 2016), the cells of microorganisms might act as precipitation templates to concentrate metal ions (such as Fe ions), resulting in the formation of metal oxides. These metal oxides may further react with dissolved Si to produce authigenic clay minerals (such as kaolinite- and glauconite-like minerals with poor crystallinity) that precipitated as coatings on the surface of cell walls (Konhauser et al., 1993; Fein et al., 2002), perhaps facilitating the preservation of cells.

Compared with authigenic clay minerals that have been highlighted, the role of detrital clays in the preservation of exceptional fossils on the early Earth has received much less attention. Despite that, evidence from observation on fossils has actually showed the important role detrital clay minerals play in the preservation of soft tissue (Wacey et al., 2014). Furthermore, some microscopic characterizations on microbial fossils suggested the important role of detrital clay minerals. Brasier et al. (2015) used transmission electron microscopy (TEM) and selected area electron diffraction (SAED) to characterize the Earth's early microbial fossils, and the results showed that the clay mineral found in the fossils were well crystallized and identified as illite or vermiculite that are of non-authigenic origin. In a recent report, Anderson et al. (2020a) identified that kaolinite was associated with Proterozoic microfossils formation using elemental mapping and synchrotron-based infrared microspectroscopy. The abovementioned results suggest the potential importance of the detrital clays suspended in water column for the fossilization or the preservation of microbial cells.

In order to clarify the effect of clay minerals on the formation and preservation of microbial fossils, some experimental studies were done, for which natural detrital clay minerals with different concentrations were added to the incubation system of microbial cells in designated conditions to simulate the reactions between clay minerals and microbes. Cyanobacteria, which commonly occurred in the Precambrian fossil record (Butterfield, 1995), was used as a representative microorganism in these experimental studies. Newman et al. (2016) demonstrated that illite particles derived from coarse sand granules in siliciclastic environments with very low clay concentrations (5.6–55.6 mg/L) contribute to cyanobacterial aggregation and encrustation. Playter et al. (2017) further showed that the addition of high concentration of clay minerals (kaolinite and montmorillonite, 5–50 g/L) into cyanobacterial culture caused the encasement of the cyanobacteria in clay and their sedimentation in a very short time (approximately 15 min). These studies suggested that clays likely facilitated microbial preservation by rapid formation of shape-preserving mineral coatings (Newman et al., 2016, 2017). The insights from these studies suggest the role of clays in microbial preservation warrants in depth investigation, specifically targeting the underpinning mechanics of microbe-clay interactions.

In this work, three clay minerals, montmorillonite, illite and kaolinite are used to investigate cyanobacteria-clay interaction and the aggregation and preservation of cyanobacteria. These minerals are recognized as representative clay minerals from perspective of the structure of clay minerals, and they commonly occur in shallow marine environments (Milliman et al., 1996) and appeared as early as 3.0 Ga ago (Hazen et al., 2013). Moreover, given the elevated concentrations of dissolved silica and metals in the Precambrian ocean (Jones et al., 2015; Tarhan et al., 2016), dissolved Si (Na_2SiO_3), Al ($NaAlO_2$ and $AlCl_3$) and Fe ($FeCl_3$) are added to seawater containing suspended clay minerals to study the effects of these species on cyanobacteria-clay aggregation.

2. Materials and methods

2.1. Cyanobacteria and clay minerals

The cyanobacterium *Spirulina maxima* was provided by the Yantai Institute of Coastal Zone Research, Chinese Academy of Sciences, Yantai, China. *Spirulina* is a filamentous cyanobacterium with multicellular spiral-shaped filaments. It belongs to the family Oscillatoriaceae, which widely occurred in seawater and fresh water and has been found in the Precambrian fossil record (Bartley, 1996; Brasier et al., 2015; Sánchez-Baracaldo, 2015). The origin of *Spirulina* has been traced to 1200–1300 Ma (Sánchez-Baracaldo, 2015; Betts et al., 2018; Sánchez-Baracaldo and Cardona, 2020).

Montmorillonite, illite and kaolinite were used in the preparation of cyanobacteria-clay co-aggregates because they are commonly found in sediments associated with microbial fossils (Milliman et al., 1996; Wacey et al., 2014; Anderson et al., 2020b). The samples of montmorillonite (Mt), illite (Il) and kaolinite (Kaol) were collected from Inner Mongolia, Jilin and Guangdong in China, respectively. Purification treatment (Liu et al., 2013) was conducted to remove the impurity minerals without disturbing the structure and properties of the clays. X-ray diffraction (XRD) patterns (Fig. S1) show that these minerals are of high purity. Their chemical compositions (mass %) are as follows: Mt. – 5.50% Na_2O, 38.67% Al_2O_3, 47.37% SiO_2, 2.04% CaO, and 6.41% Fe_2O_3; Il – 1.47% MgO, 49.38% Al_2O_3, 32.90% SiO_2, 9.70% K_2O, and 3.19% Fe_2O_3; and Kaol – 69.27% Al_2O_3, 29.38% SiO_2, 0.11% K_2O, 0.57% Fe_2O_3, and 0.68% TiO_2.

2.2. Cultivation of cyanobacteria

Cyanobacteria were cultured in ASW containing 0, 0.1, 1.0, 10 and 20 mg/L clay minerals; these concentrations were selected because they are typical in shallow marine environments (Milliman et al., 1996; Newman et al., 2016). The clay suspensions (before the cultivation of cyanobacteria) were produced by using a mild ultra-sonication treatment (40 kHz/60 W) for 60 min, which allowed the complete dispersion of clay minerals. The cultivation was conducted in 100 mL of sterilized artificial seawater (ASW; with an initial pH 8.2) in 270-mL epoxy plastic jars at 25 °C in a light growth chamber (the list of ingredients used to make the ASW is given in Table S1). The light intensity was 20 μmol photons m^{-2} s^{-1}, and a 12-h light and 12-h dark cycle was used after preliminary experiments testing the growth under different light conditions.

During cultivation, optical densities at 683 nm, 662 nm and 645 nm (denoted as OD683, 662 and 645, respectively) of the ASW-clay solution were measured at 1-day intervals by a UV-759 spectrophotometer in 1 cm cuvettes. All samples were diluted into the linear range of OD683 between 0.01 and 0.3. The conversion of OD683 to dry cell weight (DCW) (in the absence of clay) was calculated by Eq. (1), which was determined by weighting cell pellets washed three times with MilliQ filtered water and then lyophilized until a constant weight was achieved (Sinetova et al., 2012). The chlorophyll *a* (denoted as Chl-*a*) concentration was calculated by Eq. (2) (Dere et al., 1998). The above clay concentrations did not impact [Chl-*a*] measurements by comparing the OD662 and 645 of ASW during cyanobacterial cultivation in the presence or absence of clay minerals. Each experiment was in triplicate and the average value of DCW and [Chl-*a*] was used for discussion.

$$DCW = 1.27 \times OD_{683} + 0.18 \left(R^2 = 0.99\right)\ mg/mL \quad (1)$$

$$[Chl-a] = (11.75 \times OD_{662} - 2.350 \times OD_{645})\ \mu g/mL \quad (2)$$

2.3. Preparation of cyanobacteria-clay co-aggregates

The culture system in which cyanobacteria were grown in the presence of 10 mg/L clay minerals was selected for the investigation on the

aggregation between cyanobacteria and clay minerals. The clay concentration (10 mg/L) is selected by referring to previous study (Newman et al., 2016) and was tested by pre-experiments where the growth dynamics (i.e., DCW and [Chl-*a*]) of cyanobacteria in the presence of 0, 0.1, 1.0, 10 and 20 mg/L clay suspensions were investigated. The experimental settings are shown in Table S2. The cyanobacteria cultured in seawater in the absence of clay and dissolved Si, Al and Fe are taken as the control and are referred to as "Cyano group". The cyanobacteria incubated in the presence of 10 mg/L clay suspensions are referred to as the "Cyano_Clay groups", where "Clay" refers to Mt., Il or Kaol. To assess the formation of cyanobacteria-clay co-aggregates in clay suspensions, the cyanobacterial aggregates were collected for further analysis on days 1, 3 and 7.

To investigate the effects of added Si, Al or Fe on cyanobacteria-clay co-aggregation, Na_2SiO_3, $NaAlO_2$, $AlCl_3$ and $FeCl_3$ were added to the seawater containing suspended clay (10 mg/L). The concentration of the added ion was 0.3 mM, which is within the range of concentrations suggested for Proterozoic marine environments (Jones et al., 2015; Saito, 2016). The corresponding experiments are referred to as "Cyano_Clay_SiO_3^{2-}", "Cyano_Clay_AlO_2^-", "Cyano_Clay_Al^{3+}" and "Cyano_Clay_Fe^{3+}", respectively. The cyanobacteria-clay co-aggregates that formed in the presence of dissolved Si, Al and Fe were collected on days 3 and 7 for further analysis. The medium was titrated every two days with HCl or NaOH to maintain a relatively constant pH (8.0 ± 0.5) (Newman et al., 2017), even with the addition of Si, Al or Fe ions.

2.4. Microscopic and spectroscopic observations

The cultured cyanobacteria and the cyanobacteria-clay co-aggregates were observed by light microscopy (LM), scanning electron microscopy (SEM) and TEM. For the LM, 0.1 mL of culture medium containing cyanobacteria or co-aggregates was removed from the epoxy plastic jar, dropped onto slides, and observed using a light microscope (Olympus BX43). For the SEM and TEM observations, the samples were placed overnight in a 1.5-mL tube containing 1 mL of formaldehyde (25%, v/v), dehydrated using ethanol over 10 min and dried at room temperature and atmospheric pressure for 30 min. An FEI NovaTM NanoSEM 230 SEM instrument with an Oxford energy dispersive X-ray spectrometer (EDS) was used to perform the SEM observations and to determine the elemental compositions of the cyanobacteria-clay co-aggregates by selecting at least 5 spots or areas for each sample. The atomic ratios of Al to Si (denoted as Al/Si ratio) were then analyzed based on the EDS atomic compositions of each sample. An FEI Talos F200S TEM with an Oxford EDS was used to obtain the TEM, SAED and elemental mapping results. The aggregates were dried for Fourier transform infrared (FT-IR) spectroscopy using a DFZ6050 vacuum drying oven. The FT-IR spectra were recorded over 500–4000 cm^{-1} using an FT-IR spectrometer (Bruker Vertex 70) after mixing 0.9 mg of each sample with 80 mg of KBr and pressing the mixture into a pellet.

3. Results

3.1. Cultivation of cyanobacteria in clay suspensions

The cell growth of the cyanobacteria incubated in the suspension where 0–20 mg/L montmorillonite is present is shown in Fig. 1. According to the increase rate of the DCW (Fig. 1a), the growth of cyanobacteria is divided into the exponential phase and the stationary phase. The DCW increases rapidly during the exponential phase (days 0–3) and increases slowly during the stationary phase (days 4–7). The slow increase in the DCW indicates that the growth and the death of cyanobacteria reach a balance, where the biomass remains largely unchanged. During the exponential phase, variation of the DCW with different clay concentrations in the same day is small (Fig. 1a). However, during the stationary phase, the DCW roughly increases as clay concentration increases; specifically, the values of the DCW corresponding

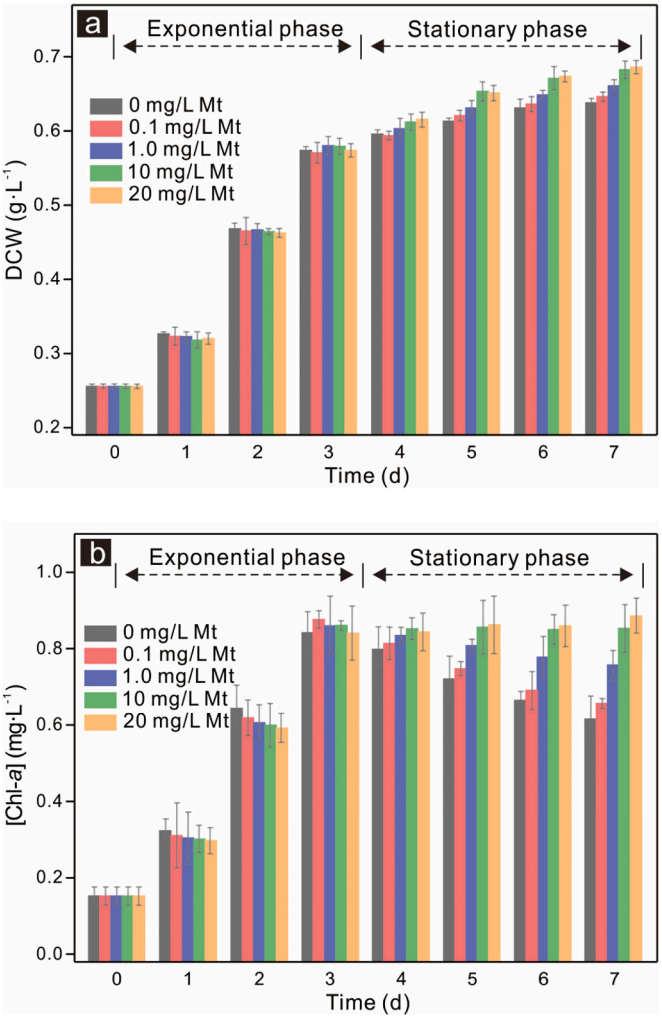

Fig. 1. Growth dynamics of cyanobacteria in the presence of 0, 0.1, 1.0, 10, 20 mg/L montmorillonite suspensions. The growth was characterized by DCW (a) and Chl-*a* concentration (b), which reflected the accumulation of biomass and the efficiency of photosynthesis, respectively.

to different montmorillonite concentrations follow the order: 20 mg/L ≈ 10 mg/L > 1.0 mg/L > 0.1 mg/L ≈ 0 mg/L.

The content of Chl-*a* in the incubation system reflects the number of the cyanobacteria that are still alive because Chl-*a* is closely related to their growth and photosynthetic activity. During the exponential phase, the [Chl-*a*] values gradually increase, and their variation with different clay concentration is small (Fig. 1b). During the stationary phase, the [Chl-*a*] values gradually decrease from day 4 to day 7 in the presence of 0.0–0.1 mg/L montmorillonite; however, such trend of [Chl-*a*] decrease is less distinct in the presence of 1.0 mg/L montmorillonite. For the groups where 10 and 20 mg/L montmorillonite are present, the [Chl-*a*] values remain almost constant on days 4–7 (Fig. 1b). Moreover, on days 4–7, the [Chl-*a*] values increase with the increase of the clay concentration (Fig. 1b), which is similar to the tendency of the change of DCW. These results indicate that relatively high concentration of suspended montmorillonite (10 and 20 mg/L) in the cyanobacteria incubation system has a significant effect on keeping cyanobacteria alive and on preventing the Chl-*a* from degradation.

Similar results of DCW and [Chl-*a*] are observed when cyanobacteria are grown in the incubation system where suspended illite or kaolinite are present (see details in Fig. S2). Briefly, the DCW and [Chl-*a*] are not affected by the addition of illite and kaolinite on days 0–3 (Fig. S2a-d); however, the addition of illite and kaolinite at high clay concentration

(10 and 20 mg/L) significantly promotes the preservation of cyanobacterial biomass and of [Chl-*a*] on days 4–7 (Fig. S2a-d). The moderately high clay concentration, 10 mg/L, was therefore adopted as the condition for the incubation experiments to observe the interactions between cyanobacteria and clays.

3.2. Formation of cyanobacterial aggregates in clay suspensions

The photomicrographs of the cyanobacteria cultured in different conditions are shown in Fig. 2. The cyanobacteria collected from the control experiment (Cyano group) are rarely aggregated (Fig. 2a and b show LM and SEM observations, respectively). The surfaces of the cyanobacteria in this group are smooth and clean, and the EDS results (Fig. 2c) indicate the presence of elements that are cellular constituents (C, O, N, P, S, Mg and K).

The cyanobacteria in the Cyano_Mt group show obvious morphological changes. After 1 day of growth, the cyanobacterial cells tend to aggregate on small scales, and some finely grained granules (with size of several microns) are occasionally observed on the surfaces of the cyanobacteria (as indicated by the blue arrow in Fig. 2d). The formation of cyanobacterial aggregates clearly occurs after only 3 days of growth (as indicated by the arrow in Fig. 2e). The cyanobacteria-clay aggregates become more distinct after 7 days of growth. The surfaces of the cyanobacterial cells in the aggregates are substantially blurred (as indicated by the arrow in Fig. 2f), which implies modification of the cell surfaces by the aggregation process.

SEM characterization enables further assessment of the morphological changes described above. Tiny granules (with size of several microns) deposited on the surfaces of cyanobacteria are observed in the Cyano_Mt group on day 1 (see the inset enlargement in Fig. 3a). As identified using EDS, there are some inorganic-organic aggregates distributed around the cells, which is indicated by the square and oval in Fig. 3a. The EDS spectrum (Fig. 3a) of the surfaces of cyanobacteria within the selected area shows the presence of Si and Al, in addition to the elements (C, O, N, P, S, Mg and K) that make up cyanobacteria. The Al/Si ratio of 0.354 ± 0.009 ($n = 5$) is similar to the Al/Si ratio (0.352 ± 0.007, $n = 5$) of the pristine montmorillonite, confirming the presence of montmorillonite in the deposited granules.

In the Cyano_Mt group, the cyanobacteria-clay co-aggregation is more distinct on day 3 than on day 1 (Fig. 3b). In the Cyano_Mt group on day 7, large-scale cyanobacteria-clay co-aggregation, in which cyanobacterial cells are closely aggregated with clay particles, is observed (Fig. 3c). Some clay particles form thick coatings on the cyanobacterial surfaces, exemplified by the place indicated by square (Fig. 3c). According to the SEM and EDS results, two forms of clay particles are present in the co-aggregates; one is represented by clay coatings on cyanobacterial cell surfaces (indicated by the dashed arrows in Fig. 3b-c); the other is the clay particles commingled with other clay particles or cyanobacterial cells in the cyanobacteria-clay co-aggregates (indicated by the solid arrows shown in Fig. 3a-c). The average Al/Si ratios of the EDS spectra for the particles occurring within the co-aggregates (Fig. 3b) and for the coated particles (Fig. 3c) are 0.362 ± 0.008 ($n = 5$) and 0.371 ± 0.010 ($n = 5$), respectively.

The TEM analyses of the cyanobacteria-clay co-aggregates in the Cyano_Mt group (Fig. 4a, Fig. S3 and S4) confirm the presence of the two types of clay granules revealed by LM and SEM. The TEM observations shown in Fig. 4a indicate that, in addition to clay granules that occur as coatings adhering closely to cyanobacterial surfaces, clay granules that fill in the areas among cyanobacterial cells and loosely link the cyanobacteria are also present in the co-aggregates on day 3 (indicated by the top-right rectangle in Fig. 4a).

EDS mapping (Fig. 4b) shows the loosely linked clay aggregates in the co-aggregates contain abundant C and N, in addition to Si and Al, suggesting that these clay granules contain cyanobacterial organic matter. EDS mapping (Fig. 4c) of the border area (indicated by the bottom rectangle in Fig. 4a) between two cyanobacterial cells reveals that the cell surfaces also contain ample Al, Si, O and C. In particular, at the places where a pair of cells is in direct contact (Fig. 4c), the contents of Al and Si are even higher than other places on the cyanobacterial surfaces.

Similarly, TEM and EDS analyses of cyanobacteria-clay co-aggregates in the Cyano_Mt group on day 7 (Fig. S4) show that the clay aggregates that occur in the co-aggregates contain abundant cyanobacterial organic matter, and that the contact region contains

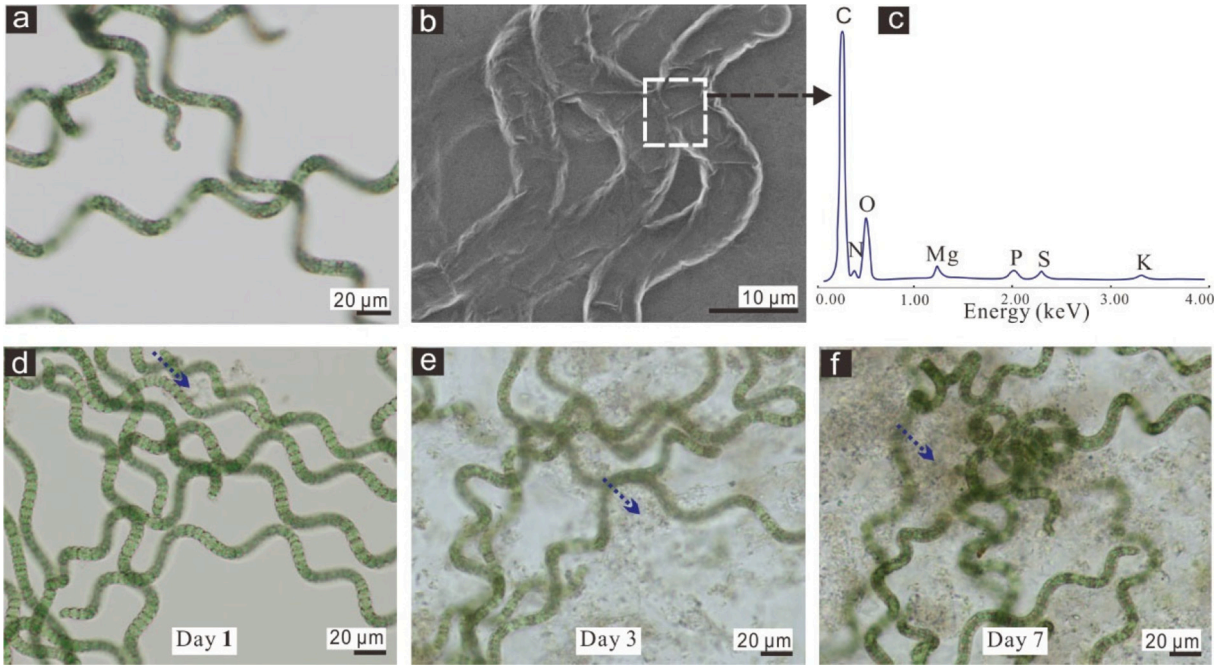

Fig. 2. LM (a) and SEM (b) images and the results of EDS analysis (c) of cyanobacteria in the Cyano group and LM images of cyanobacterial aggregates in the Cyano_Mt group on days 1 (d), 3 (e) and 7 (f). The EDS analysis (c) of the selected area (white rectangle) in panel (b) reflects the occurrence of C, O, N, P, S, Mg and K. The arrows in (d), (e) and (f) indicate the spread of tiny granules (with size of several microns) in the aggregates.

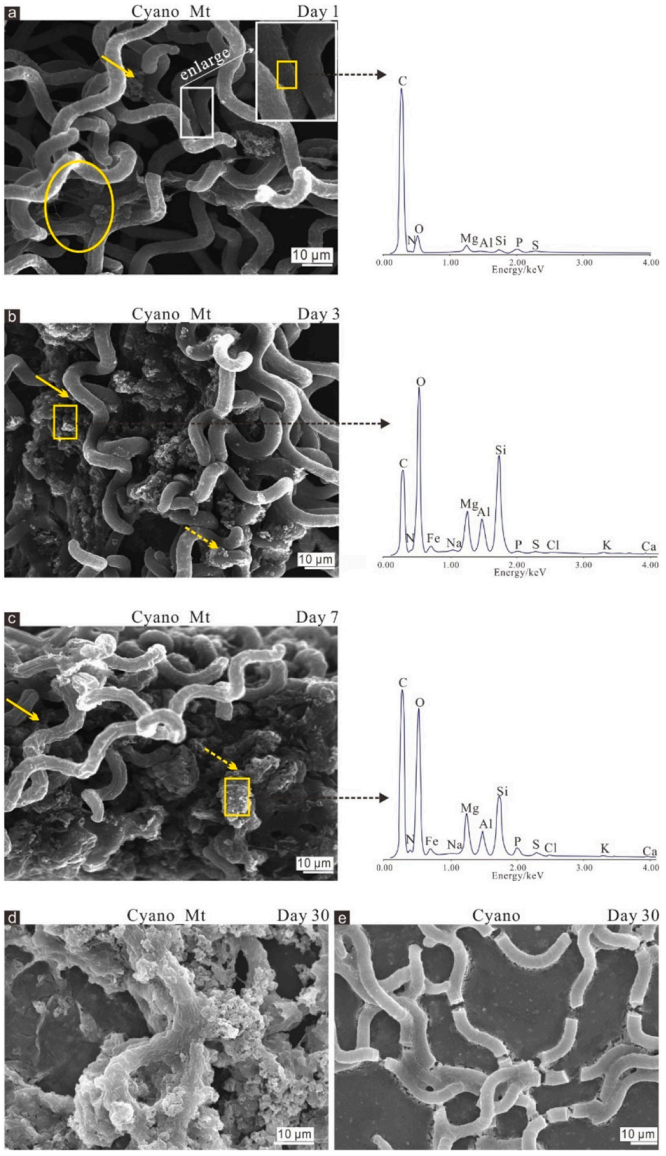

Fig. 3. SEM images of cyanobacteria-clay co-aggregates in the Cyano_Mt groups on day 1 (a), day 3 (b), day 7 (c) and day 30 (d), and cyanobacteria in Cyano group on day 30 (e). The image in the top right corner of panel (a) shows an enlargement of the selected area. The dashed arrows indicate particles that occur as coatings on the surfaces of cyanobacteria. The solid arrows indicate particles that fill in the spaces among cyanobacterial cells. The oval indicates the sticky organic matter produced by the cyanobacteria. The yellow squares denoted selected areas analyzed using EDS. Panels (d) and (e) show that the cyanobacteria in the Cyano_Mt group are still well-preserved after 1-month cultivation of cyanobacteria, while the cyanobacteria in Cyano group were broken. (For interpretation of the references to colour in this figure legend, the reader is referred to the web version of this article.)

large amounts of clay minerals.

The SAED patterns of the clay minerals that make up the co-aggregates in the Cyano_Mt group on days 1 (Fig. S3b), 3 (Fig. 4b) and 7 (Fig. S4a) show that the (100) diffractions of montmorillonite are 0.4124 nm, 0.4107 nm and 0.4090 nm, respectively. These values are slightly lower than that of pristine montmorillonite ($d_{100} = 0.4149$ nm) (Fig. S5).

A similar pattern of cyanobacteria-clay co-aggregation with increasing cyanobacterial growth time increases is observed in the systems in which illite or kaolinite were used. Briefly, some small granules deposited on the cyanobacterial surfaces are occasionally observed in the Cyano_Il group and the Cyano_Kaol group on day 1 (Fig. S6a and Fig. S6d, respectively), whereas the formation of cyanobacterial aggregates is clearly seen on day 3 (Fig. S6b, e) and is even more distinct on day 7 (Fig. S6c, f). The aggregates in the Cyano_Il and Cyano_Kaol groups also contain two types of granules (Fig. S7a-c). The Al/Si ratios of the granules in the Cyano_Il and Cyano_Kaol groups are 0.684 ± 0.018 ($n = 5$) and 1.058 ± 0.019 ($n = 5$), respectively; these values are slightly higher than those of the pristine illite (0.672 ± 0.015, $n = 5$) and kaolinite (1.055 ± 0.018, $n = 5$).

The FT-IR spectra of the pristine clay minerals and of the cyanobacteria in the Cyano group are shown in Fig. 5a. All the pristine clays show typical vibrations that correspond to the referenced clay minerals (Madejová et al., 1998; Madejová, 2001; Djomgoue and Njopwouo, 2013), and the vibrations of the cyanobacteria in the Cyano group are similar to those that have been previously reported (Yee et al., 2004; Haghighi et al., 2017). The assignments for the vibrations are summarized in Table 1.

3.3. *Effects of added Si, Al and Fe on the formation of cyanobacteria-clay co-aggregates*

In the presence of dissolved Si, Al and Fe ions, very strong aggregation occurs between cyanobacterial cells and clay particles. This process is exemplified by the SEM observations of the Cyano_Mt_ SiO_3^{2-}, Cyano_Mt_AlO_2^-, Cyano_Mt_Al^{3+}, and Cyano_Mt_Fe^{3+} groups on day 7 shown in Fig. 6; the cyanobacterial cells are so closely associated with the clay particles that the filamentous structure of the cyanobacteria is almost unresolvable in the aggregates (indicated by the dashed arrows shown in Fig. 6a-d). Visible differences occur in the structure of the aggregates that are produced under different ions, as seen in the SEM images (Fig. 6a-d). For example, the surfaces of the cyanobacteria are completely coated with clay in the samples in the Cyano_Mt_AlO_2^- (Fig. 6b), Cyano_Mt_Al^{3+} (Fig. 6c), and Cyano_Mt_Fe^{3+} (Fig. 6d) groups; however, the microstructures (as indicated by features such as smoothness and texture) of the surface coatings are quite different. The co-aggregates in the Cyano_Mt_Al^{3+} group exhibit a nest-like texture that contains some pores (Fig. 6c), and the coatings in the Cyano_Mt_Fe^{3+} group show a relatively smooth and uniform distribution (Fig. 6d).

The EDS results of the selected areas shown in Fig. 6a-d quantify the differences in the cyanobacteria-clay co-aggregates that are produced in the presence of different added ions. The EDS spectra show that the contents of Si, Al, Al and Fe atoms in the co-aggregates in the Cyano_Mt_SiO_3^{2-} (Fig. 6a), Cyano_Mt_AlO_2^- (Fig. 6b), Cyano_Mt_Al^{3+} (Fig. 6c) and Cyano_Mt_Fe^{3+} (Fig. 6d) groups are significantly higher than those of Mt. (Fig. 3c). The increases in the abundances of these species in the co-aggregates when the relevant compounds are added to the Cyano_Mt group indicate that these ions can enter the co-aggregates. The SEM and EDS analyses yield similar results for the groups of experiments performed using other clay minerals (illite and kaolinite) (Fig. S8).

The Al/Si and Fe/Si ratios of the clay minerals in co-aggregates in the presence of added ions show noticeable variations (Fig. 7). The Al/Si ratios of the co-aggregates in the Cyano_Clay_SiO_3^{2-} groups on days 3 and 7 (Fig. 7a) are significantly lower than those of the pristine clays due to the introduction of SiO_3^{2-}, which results in an increase in Si. However, the Al/Si ratios are higher on day 7 than on day 3, indicating that the addition of SiO_3^{2-} permits an increase in the clay content in the co-aggregates by day 7 and thereby increases the Al/Si ratio. For the case of other added ions, the Al/Si ratios of the Cyano_Clay_AlO_2^- (Fig. 7b) and Cyano_Clay_Al^{3+} (Fig. 7c) groups on days 3 and 7 and the Fe/Si ratios of the Cyano_Clay_Fe^{3+} (Fig. 7d) group on days 3 and 7 also suggest that the added AlO_2^-, Al^{3+}, and Fe^{3+} is rapidly introduced into the co-aggregates and increases the contents of clay minerals.

The FT-IR characteristics of the cyanobacteria-clay co-aggregates in the groups that contain added ions (Fig. 8a-d) are different from those in

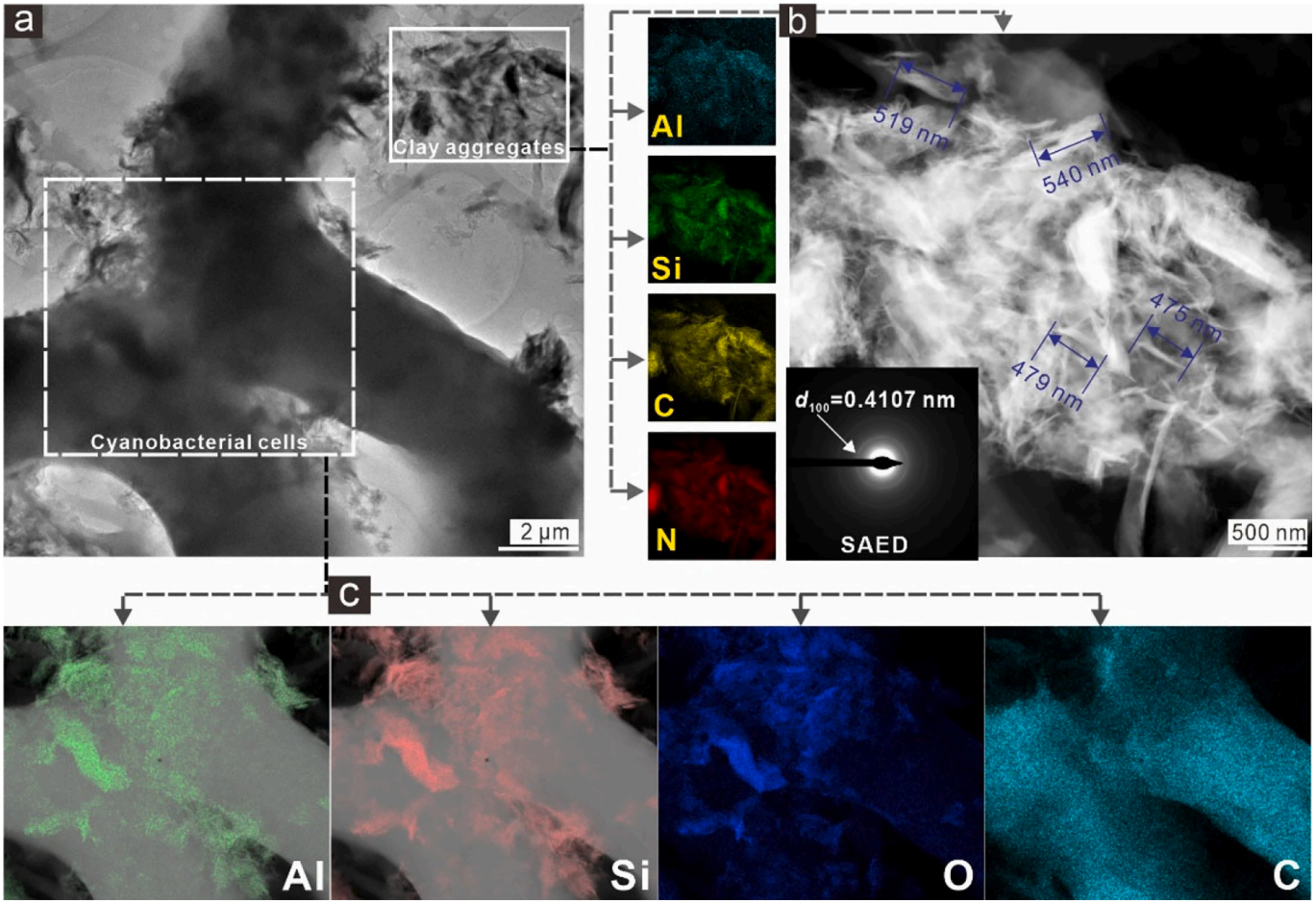

Fig. 4. TEM image (a), SAED patterns (b) and elemental distributions (b, c) of cyanobacteria-clay co-aggregates in the Cyano_Mt group on day 3. The TEM image in panel (a) shows two cells in contact with one another (indicated by the rectangle on the left) and a clay aggregate (indicated by the rectangle in the upper right). Panel (b) shows the SAED patterns and Al/Si/C/N distribution of the selected area shown in panel (a); the sizes of the montmorillonite grains range from 475 to 540 nm. Panel (c) shows the Al/Si/O/C distributions of the contact area of the cyanobacteria-clay co-aggregate shown in panel (a).

their absence (Fig. 5b). The —COOH band (1260 cm^{-1}) still appears in the groups that contain added ions, although its intensity is low. Meanwhile, the intensity of the $—COO^-$ band (1413 cm^{-1}) is weaker in the Cyano_Clay_SiO_3^{2-} (Fig. 8a), Cyano_Clay_AlO_2^- (Fig. 8b), Cyano_Clay_Al^{3+} (Fig. 8c) and Cyano_Clay_Fe^{3+} (Fig. 8d) groups than in their counterparts that do not contain added ions. In addition, the Al—OH band (3695 cm^{-1}) of the cyanobacteria-clay co-aggregates is much less intense in the groups that contain added ions than in their counterparts that do not contain added ions.

4. Discussion

4.1. Role of clay minerals in the cyanobacteria-clay co-aggregation

The results described above clearly demonstrate that the presence of low-concentration (10 mg/L) suspended clay minerals in the growth environments of cyanobacteria plays a key role in the cyanobacteria-clay co-aggregation. As indicated by the FT-IR spectra, the characteristic bands of the cyanobacteria-clay co-aggregates (Fig. 5b) display obvious differences when compared to those of the pristine clay minerals and cyanobacteria (Fig. 5a). For the Cyano_Mt group, the —CH stretching vibration for fatty acids (at 2932 cm^{-1}), the C═O stretching vibration for protein amide I (at 1658 cm^{-1}) and the N—H bending vibration for protein amide II (at 1546 cm^{-1}) are shifted toward higher wavenumbers than those of the Cyano group. Moreover, the broad band of C—OH bending for saccharide (at 1045 cm^{-1}) overlaps with the Si—O stretching band of montmorillonite (at 1036 cm^{-1}). The distinct shift in or disappearance of the vibrations associated with lipids, proteins, and saccharides in the spectra of the Cyano_Mt group compared with those of the Cyano group indicates that these organic compounds are involved in the formation of cyanobacteria-clay co-aggregates. Notably, it has been reported that the carboxyl groups existed in EPS or at the cell surface of cyanobacteria to maintain the cells alive in the pH range (8.0 ± 0.5) of the culture experiment (Yee et al., 2004; Dittrich and Sibler, 2005; Haghighi et al., 2017). However, the band associated with the —COOH of organic matter at 1260 cm^{-1} disappears after the aggregation of montmorillonite and cyanobacteria, and the intensity of the characteristic band associated with $—COO^-$ (at 1413 cm^{-1}) greatly increases accordingly, suggesting the deprotonation of the surfaces of the cyanobacterial cells (Yee et al., 2004). On the other hand, a distinct change occurs in the vibration of the hydroxyl groups of montmorillonite. An intense band appears at 3695 cm^{-1} in the spectrum of the Cyano_Mt group; it is a typical stretching vibration of Al—OH, which does not occur in the spectrum of montmorillonite (Fig. 5a). Both phenomena suggest that the —COOH group participates in the process that results in the formation of Al—OH in montmorillonite. In addition, the reduction in the intensity of the vibrations of Al—O—Si (at 519 cm^{-1}) suggests the breakage of Al—O—Si bonds of montmorillonite (Madejová et al., 1998).

The interactions between the surface groups of clay minerals (Lagaly and Dékány, 2013) and those of cyanobacteria (Martinez et al., 2008) can effectively explain the observed cyanobacteria-clay co-aggregation.

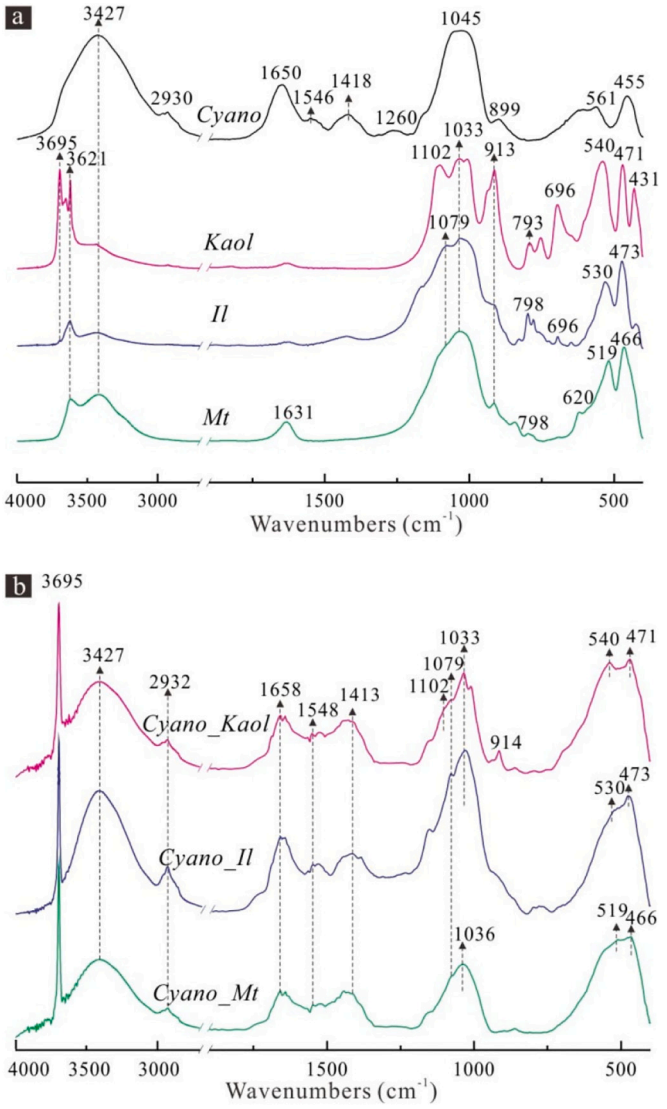

Fig. 5. FT-IR spectra of pristine clay minerals and cyanobacteria in the Cyano group (a) and the spectra of cyanobacteria-clay co-aggregates in the Cyano_Mt, Cyano_Il and Cyano_Kaol groups.

The surfaces of living cyanobacterial cells are generally negatively charged over a wide range of pH values due to the large amounts of anions (Martinez et al., 2008), such as $—COO^-$ and $—HCO_3^-$, distributed over the cyanobacterial surfaces to support photosynthesis. Despite the presence of this overall negative charge, some of the surface positions on cyanobacteria may be positively charged because the groups found in some proteins (such as $—NH_2$) readily transform into protonated aminopropyl groups ($—NH_3^+$) in aqueous solutions. This heterogeneity of the surface charges of cyanobacterial surfaces has been investigated in detail (Dittrich and Sibler, 2005). Additionally, the type and distribution of the surface charges of clay minerals in aqueous solutions have frequently been investigated. As an example, a montmorillonite particle contains two different surfaces from a surface charge perspective (Lagaly and Dékány, 2013). One is the basal surface (referred to as the "face" hereafter; Fig. 9a), which has a permanent negative charge that arises from the isomorphous substitution of Al^{3+} for Si^{4+} in the tetrahedral sheet of montmorillonite. The other surface is the edge surface (here shortened to the "edge"; Fig. 9a), which has a variable charge that depends strongly on the ambient pH. The charge at the edge arises from the adsorption or dissociation of protons by the hydroxyl groups (silanol and/or aluminol, denoted as *>SOH*), as is also seen in oxides (Lagaly and Dékány, 2013). Under acidic conditions, an excess of protons promotes the protonation of the surface and creates positive edge charges (Eq. (3)), the density of which decreases as the pH increases. In contrast, the dissociation of silanol and aluminol groups at relatively high pH values produces negative charges (Eq. (4); Tournassat et al., 2004). Consequently, the $>SOH_2^+/>SO^-$ ratio at a certain pH has a decisive effect on the overall surface charge.

Table 1
Assignments of FT-IR vibrational bands to the main absorption peaks seen in Fig. 5. The assignments of the bands are made on the basis of previous publications (Madejová, 2001; Yee et al., 2004; Djomgoue and Njopwouo, 2013; Haghighi et al., 2017).

Samples	Wavenumbers (cm^{-1})	Assignment
Pristine clays	3695	—OH stretching due to the coordination of hydroxyl groups with octahedral Al^{3+} cations
	3621	—OH stretching of inner hydroxyl groups
	3427	—OH stretching of water
	1102, 1079, 1033	Si—O stretching
	913	Al—OH stretching of inner hydroxyl groups
	798, 793	Si—OH stretching
	540, 530, 519	Al—O—Si bending
	473, 471, 466	Si—O—Si bending
Cyano group	3427	—OH stretching of water
	2930	—CH stretching of lipids
	1650	C═O stretching of protein amide I
	1546	N—H bending of protein amide II
	1418	C═O stretching of $—COO^-$ due to the formation of deprotonated carboxyl surface sites
	1260	C—O stretching of —COOH
	1045, 899	C—OH bending (dominated by saccharides)
	455	—S—S— bending

$$> SOH + H^+ => SOH_2^+ \quad (3)$$

$$> SOH => SO^- + H^+ \quad (4)$$

Owing to the features of the surface charges of cyanobacteria and montmorillonite particles mentioned above, the montmorillonite particles are readily attracted by cyanobacteria through electrostatic attraction between oppositely charged cyanobacteria and montmorillonite surfaces. Examples include $—NH^{3+}$-face(−) contact and $—COO^-$(or HCO_3^-)-edge(+) contact. As a result, cyanobacteria-clay co-aggregation is initiated once the surfaces of cyanobacterial cells begin to be coated by montmorillonite particles (evidenced by Figs. 2–3); the coating very likely acts as a bridge and mediates the link between cyanobacterial cells, then restricts the mobility of the cyanobacteria and finally leads to a loss of the ability to escape from further coating or encrustation by montmorillonite particles on the part of the cyanobacteria. This point is evidenced by the increased content of Al and Si in the contact region shown in Fig. 4c. The coating of montmorillonite particles on cyanobacterial surfaces may in turn accelerate the co-aggregation of clay-coated cyanobacterial shells. As well demonstrated previously, clay particles readily and spontaneously form aggregates in aqueous solutions (Lagaly and Dékány, 2013). These aggregates form either so-called "house-of-cards" networks that are joined by edge-face contacts and are preferred in acidic conditions or band-type networks that are joined by face-face contacts and frequently occur under relatively high pH conditions (Lagaly and Dékány, 2013). Thus, larger amounts of suspended clay particles form co-aggregates to be incorporated into the cyanobacterial shells through edge-face or face-face aggregation of clay particles. The formation of cyanobacteria-clay co-aggregates may further limit the mobility of cyanobacteria and possibly stop photosynthesis via blocking off sunlight, resulting the inclusion of more clay particles and thus forming stable and thick co-aggregates (schematically represented in Fig. 9b).

For the Cyano_Il and Cyano_Kaol groups (Fig. 5b), the shifts in the vibrations at 2932 cm^{-1}, 1658 cm^{-1} and 1548 cm^{-1} also reflect

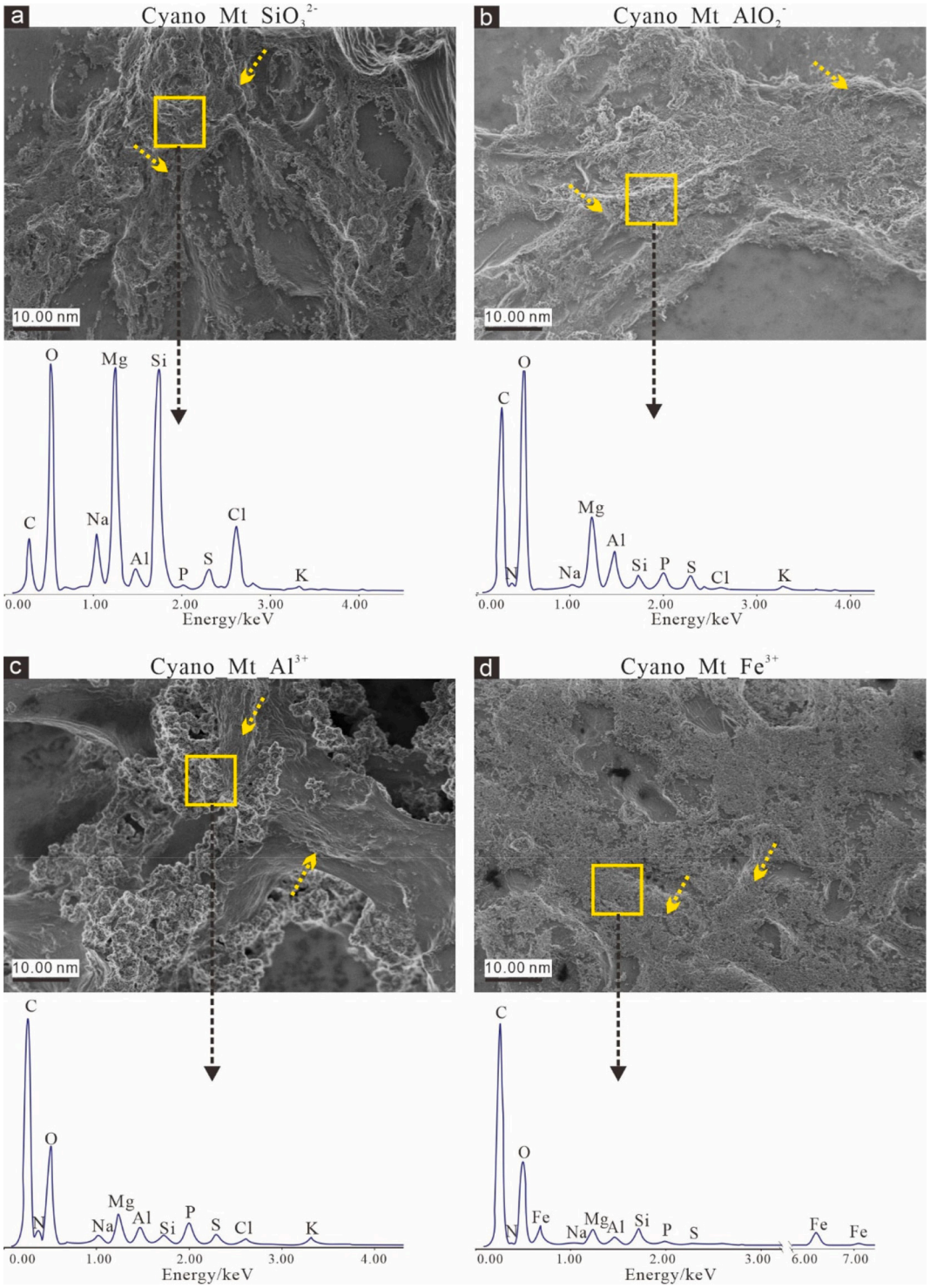

Fig. 6. SEM images and EDS spectra of cyanobacteria-clay co-aggregates in the Cyano_Mt_SiO_3^{2-} (a), Cyano_Mt_AlO_2^- (b), Cyano_Mt_Al^{3+} (c) and Cyano_Mt_Fe^{3+} (d) groups on day 7. The dashed arrows indicate cyanobacterial cells.

interactions between cellular organic matter (lipids, proteins and saccharides) and the clays. Moreover, the increase in the intensities of the vibrations at 1413 cm^{-1} and the disappearance of the vibrations at 1260 cm^{-1} suggest the deprotonation of the surfaces of the cyanobacterial cells, and the appearance of a distinct peak at 3695 cm^{-1} indicates the formation of new Al—OH groups in the Cyano_Il, as also occurred in the Cyano_Mt group mentioned above. The partial breakage of Al—O—Si bonds in the Cyano_Il and Cyano_Kaol groups is indicated by the reduction in the intensity of the 530 cm^{-1} band (in the Cyano_Il group) and the disappearance of the band at 540 cm^{-1} (in the Cyano_Kaol group). Overall, illite and kaolinite have surface charge features that are comparable to those of montmorillonite, although their amounts of permanent negative charge and their proportions of silanol groups are different (Brigatti et al., 2013; Emmerich, 2013). All these clay minerals have a negatively charged surface, so the co-aggregation behaviors of them are similar, and the occurrence of cyanobacteria-clay co-aggregation may be independent of the types of clay minerals that are present in suspension. Therefore, it is likely that any clay minerals that are

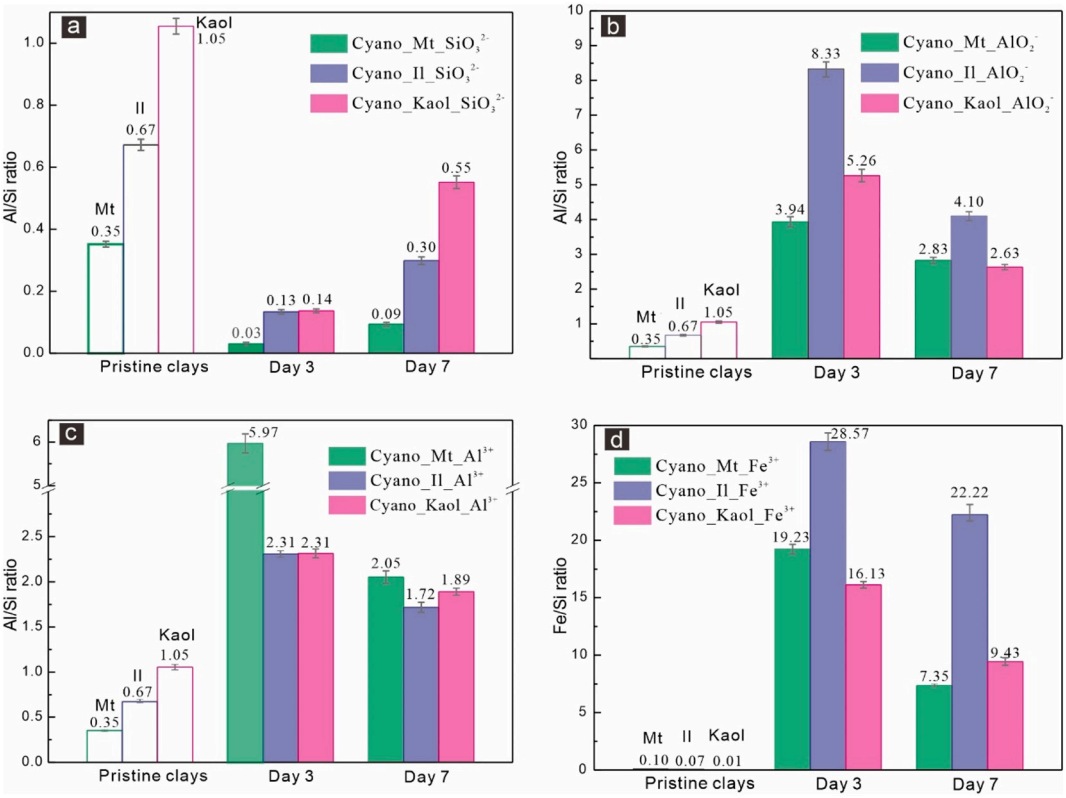

Fig. 7. Surface Al/Si ratios of cyanobacteria in the Cyano_Clay_SiO_3^{2-} (a), Cyano_Clay_AlO_2^- (b), Cyano_Clay_Al^{3+} (c), and Fe/Si ratios in Cyano_Clay_Fe^{3+} (d) groups on days 3 and 7. The Al/Si and Fe/Si ratios of pristine clay minerals are also presented in each panel to show their differences relative to each group of experiments. The Al/Si and Fe/Si ratios are calculated by analyzing the elemental compositions of the selected areas shown in Fig. 6 and Fig. S8.

common in marine environments, such as mixed-layer illite-smectite and chlorite (Madejová, 2001; Petrovich, 2001), would possess the capacities to form co-aggregates with cyanobacteria, and cyanobacteria-clay co-aggregation might be a widespread and frequently occurring process in saline waters with suspended clay minerals.

The fact that all the clay minerals (montmorillonite, illite and kaolinite) in the cyanobacteria-clay co-aggregates have similar Al/Si ratios, particle sizes and microstructures as the pristine clay minerals suggests that the clays in the co-aggregates are derived from the pristine clay suspended in the culture medium. Notably, the co-aggregation of cyanobacteria and high-concentration clay minerals had also been investigated previously. Playter et al. (2017) showed that the addition of 5 g/L or 50 g/L montmorillonite or kaolinite to a suspension of *Synechococcus* cells significantly increased the cyanobacteria-clay co-aggregation and sedimentation and cells were settled down from the suspension within 15 min. Unlike the above-mentioned conditions, this work adopts much lower concentrations of clay minerals (10 mg/L), within the scope of the suspended clay concentration in shallow marine environments (Milliman et al., 1996; Newman et al., 2016), and has been used in a recent study focusing on cyanobacteria-illite co-aggregation (Newman et al., 2016). Under such a relatively low clay concentration, cyanobacteria-clay co-aggregation occurred in 7 days, which is much slower than reported by Playter et al. (2017).

Notably, the extracellular polymeric substances (denoted as EPS) on cyanobacterial surfaces include various types of organic compounds (such as saccharides, proteins, lipids, and nucleic acids). Saccharides have been regarded as key organic compounds that react with metal ions or minerals because they are sticky and can induce the adsorption of ions or minerals onto cyanobacteria (Santschi et al., 1998; Tang et al., 2014). The present work suggests that fatty acids and proteins are also able to contribute to the cyanobacteria-clay co-aggregation by enhancing the electrostatic attraction of clay surfaces to cyanobacteria due to their —COOH and/or —NH_3 groups. In other words, the actual interfacial interactions between cyanobacteria and clay minerals are likely to be highly diverse and complex. Therefore, to specify the mechanisms of the cyanobacteria-clay interface reactions is important for understanding biogeochemical processes in early Earth environments and needs further investigation.

4.2. *Effects of dissolved Si, Al and Fe on the cyanobacteria-clay co-aggregation*

The pronounced enhancement of the cyanobacteria-clay co-aggregation in the presence of dissolved metal cations (Al^{3+} and Fe^{3+}) or anions (SiO_3^{2-} and AlO_2^-) demonstrates that dissolved metal cations and anions facilitate co-aggregation (Fig. 7). The addition of these ions to suspensions of cyanobacteria and clay minerals modifies the surface charges of the cyanobacteria and/or clay minerals, indicated by the zeta potential changes (detailed in Fig. S9), and thus lowers the stability of the suspensions. The addition of ion species at certain concentrations to diluted clay dispersions has been found to promote the aggregation of clay particles (Ma, 1997). The adsorption of metal cations to the surfaces of clay mineral grains can neutralize the permanent negative charge at the basal surface; such cations can also react with the >SO^- groups on the edges through electrostatic attraction, making the edges more positively charged. Consequently, the edge(+)-face(−) contact is strengthened, and aggregation occurs more readily. The addition of anions may react with the >SOH_2^+ groups at the edge surface, thus making the edge surface more negatively charged and enhancing the possibility of aggregation via face(−)-face(−) contact. The cyanobacteria-clay dispersion is similar to clay dispersion from some perspectives because both cyanobacteria and clay minerals are overall negatively charged with positive charges at certain surface positions.

Furthermore, the variations in the Al/Si ratios among the different

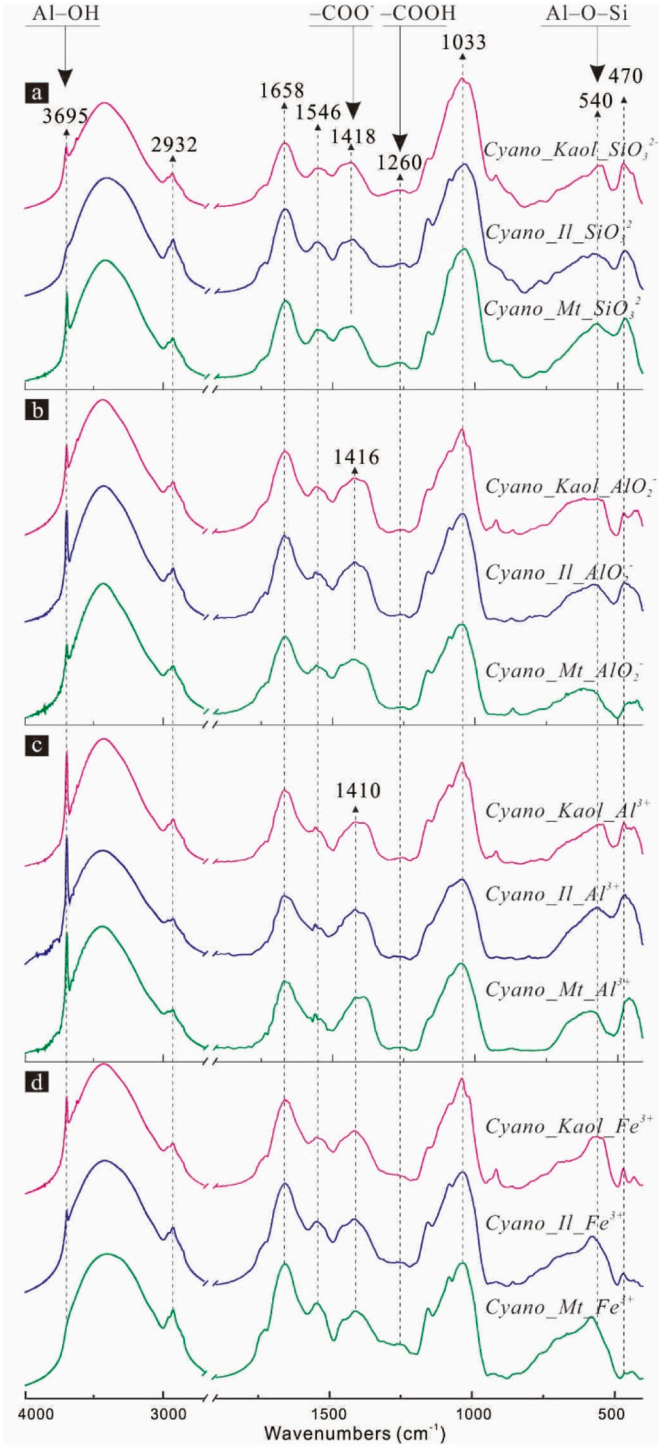

Fig. 8. FT-IR spectra of cyanobacterial aggregates in the Cyano_Clay_SiO_3^{2-} (a), Cyano_Clay_AlO_2^- (b), Cyano_Clay_Al^{3+} (c) and Cyano_Clay_Fe^{3+} (d) groups.

cyanobacteria-clay systems indicate the dependence of co-aggregation behaviors on the types of ions added, the type of clay minerals in suspension and the culture time. In the system in which cyanobacteria were cultured for 3 days in the presence of Na_2SiO_3, significant decreases in the Al/Si ratios in the cyanobacteria-clay co-aggregates are noted (Fig. 7a); these ratios are 11.7, 5.2, and 7.5 times lower than the typical Al/Si ratios of pristine montmorillonite, illite and kaolinite, respectively. The sudden increase in the Si content in the co-aggregates during the initial stage of cultivation indicates that strong adsorption of SiO_3^{2-} occurred before the occurrence of large-scale co-aggregation, demonstrating the ability of SiO_3^{2-} to promote cyanobacteria-clay co-aggregation. The addition of AlO_2^- adversely affects the Al/Si ratios on day 3 (Fig. 7b), indicating the rapid incorporation of Al into the co-aggregates. The Al/Si ratio on day 7 is lower than that on day 3 (Fig. 7b), suggesting the increasing incorporation of clay particles into the co-aggregates with increasing growth time. The initial incorporation of metal cations into the cyanobacteria-clay co-aggregates, followed by the incorporation of larger amounts of clay particles, are also noticeable in the cases in which Al^{3+} and Fe^{3+} are added (Fig. 7c and d). All the above results indicate that the presence of dissolved metal cations or anions significantly promotes cyanobacteria-clay co-aggregation.

4.3. Implications for cyanobacterial preservation and related geochemical processes

The ready cyanobacteria-clay co-aggregation in clay-rich environments and the good preservation of the cyanobacteria in the aggregates suggest that the presence of suspended clay minerals in is a key variable in the sedimentation and subsequent preservation of cyanobacteria, supporting the findings of previous studies (Newman et al., 2016, 2017; Playter et al., 2017). Of particular interest is that the cyanobacteria-clay co-aggregation is able to prevent the cyanobacterial organics (such as Chl-*a*) from decomposition, which promotes the preservation of cyanobacteria. After a long cultivation time (1 month) of cyanobacteria, the cyanobacteria in the Cyano_Mt group are still well-preserved (Fig. 3d), while the cyanobacteria in Cyano group were degraded (Fig. 3e). This result indicates that cyanobacteria-clay co-aggregation has protected the cyanobacterial organic materials inside the aggregates and increased the likelihood that cyanobacteria would be damaged by external factors such as ultraviolet radiation and biological disturbance.

The encrustation of microbial cells by metal oxides (such as iron oxide or aluminum oxide) and/or silica has been thought as a crucial stage in the aggregation of microbial cells (Gauger et al., 2016), and this process is regarded important to the preservation and fossilization of microbes. The reason is that the coating of authigenic clay minerals resulting from the recrystallization of metal oxides (Konhauser et al., 1993; Fein et al., 2002) might facilitate resisting diagenesis and/or metamorphism by cells and biostructures (Yee et al., 2003; Li et al., 2013; Gauger et al., 2016). It is likely the coating of detrital clays on the surface of cyanobacteria in co-aggregation is also beneficial for the long-term preservation of cyanobacteria. The present work demonstrates that clay coating of cyanobacteria can be from the interaction between suspended detrital clay in ambient environment and cyanobacteria, without the involvement of iron (or silicon) oxides. This is consistent with the observation of the non-authigenic origin of the clay minerals in some of Earth's early microbial fossils (Brasier et al., 2015). Therefore, this work suggests that the environments where cyanobacteria and suspended detrital clays coexist in marine environments are conducive to the sedimentation and preservation of microbes and thus may have made contributions to the microbial fossilization. However, it is unclear whether these co-aggregates would preserve the detailed cellular morphology necessary to make fossils that can be recognized as cyanobacteria; further work on the morphology of these aggregates and if and how it could be comparable to the organisms/fossils in geological records needs to be done in future.

Compared to clay minerals, silica and metal cations dissolved in water exert relatively minor controls on the rapid formation of cyanobacteria-clay co-aggregates; cyanobacteria-clay co-aggregation occurs even in the absence of added ions (Figs. 2–3, and Figs. S6–S7). Moreover, in the control experiments in which only Si, Al or Fe ions (even at high concentrations) are added, the degree of cyanobacterial encrustation is weaker than that observed in the presence of both clay minerals and dissolved ions (Fig. S10). Notably, there were broad ranges of concentrations of ions in ancient marine environments; for example, the inferred Si concentrations range from 0.1 mM to 2.2 mM, and those of Fe and Al range from 0.04 mM to 1 mM and from 0.02 to 0.4 mM,

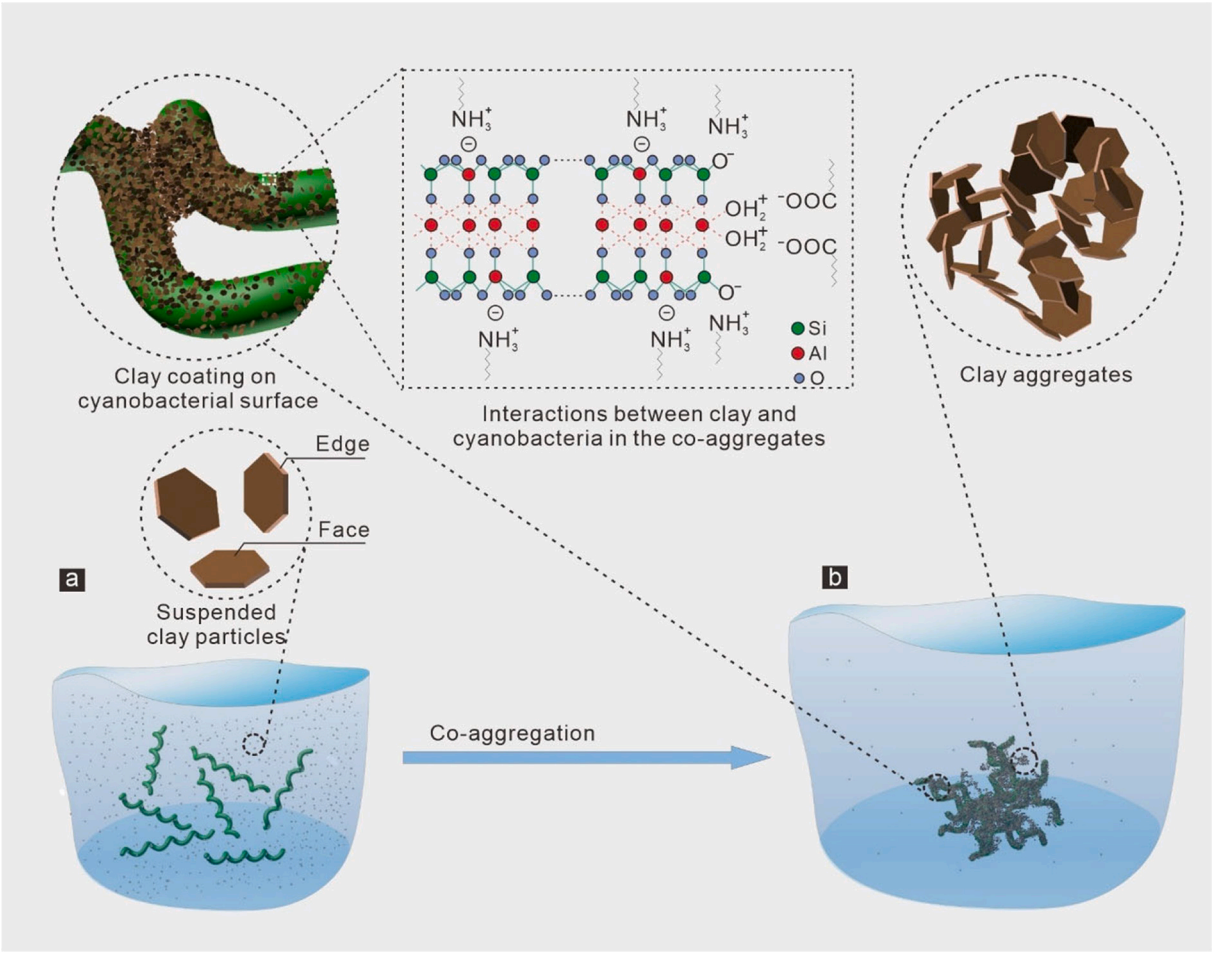

Fig. 9. Possible modes of cyanobacteria-clay co-aggregation. (a) Free cyanobacterial cells incubated in seawater in the presence of suspended clay minerals; an enlargement of clay particles shows its "face" and "edge" surfaces. (b) Cyanobacteria-clay aggregates after several days of incubation; the left enlargement shows clay particles coating on cyanobacterial surfaces and on the contact region between cyanobacterial cells, the right enlargement shows clay aggregates filling the interspaces between cyanobacterial cells, and the middle rectangle shows the possible interactions between clay and cyanobacteria in the co-aggregates (taking montmorillonite as an example).

respectively (Goldberg and Arrhenius, 1958; Gehlen et al., 2002; Jones et al., 2015; Saito, 2016; Gauger et al., 2016).

An unexpected but profound consequence of cyanobacteria-clay co-aggregation is the release of structural elements from clay minerals. This is evidenced by the slightly higher Al/Si ratios of clay minerals on day 3 and day 7 than that of pristine clay and the decrease in the d_{100} of montmorillonite (Fig. 4 and S4–5). According to the FT-IR results, the dissolution of clay might be due to the locally acidic environment, resulting from the H^+ released from reactions such as the deprotonation of —COOH of cyanobacteria. Under the acid attack, disconnection of the original tetrahedral SiO_4 and octahedral AlO_6 sheets in the montmorillonite occurs, and the Al—O—Si bonds are broken, indicated by the reduction in the intensity of the vibrations of Al—O—Si (at 519 cm^{-1}) (Madejová et al., 1998). As a result, the separated tetrahedral SiO_4 units may become unstable and are readily dissolved into solution. Therefore, the interaction between cyanobacterial cells and clays is able to liberate a small proportion of the structural Si of clay minerals. Such structural changes of clay minerals induced by cyanobacteria are confirmed also by control experiments (see details in part VII of the Supplementary data; Fig. S11a, b), in which pristine clay minerals were placed in seawater for a month in the absence of cyanobacteria and showed no structural changes. This previously unexplored cyanobacteria-induced dissolution of clay minerals might provide Si for the relevant biogeochemical Si cycles (such as the growth of diatoms). It should be considered in investigation of related geochemical processes because the coexistence of cyanobacteria and clay minerals is widespread in marine environments. This finding is of particular significance because it is well known that clay minerals are chemically inert in seawater due to their slow dissolution rates at high salinity (Jeandel and Oelkers, 2015).

Finally, the cyanobacteria-induced dissolution of clays is affected by co-existing metal ions. As seen from the FT-IR results (Fig. 8), the breakage of Al—O—Si bonds in the clays was substantially inhibited by the adsorption of added ions to the clays. The intensity of the Al—OH band (3695 cm^{-}) resulting from the breakage of Al—O—Si bonds for the groups that contain added ions is much less intense than in their counterparts that do not contain added ions (Fig. 5 and Fig. 8). The adsorption of the added ions prevents the surface reactive sites of clay minerals from interacting with —COOH groups and thereby reduces the degree of structural changes in the clay particles. The interaction between —COOH groups and metal cations can be excluded because such interaction is very weak (Fein et al., 1997; Wightman and Fein, 2005). Therefore, the cyanobacteria-clay co-aggregation not only matters to the preservation of cyanobacteria, but has potentially important but complex (e.g., sensitive to co-existing metal cations) impacts on the geochemical Si cycle in marine environments and thereby warrants further study in the future.

5. Conclusions

Clay minerals are an important component of sedimentary

environments and suspended clay minerals occur ubiquitously in the marine water column. The present work identifies the significant contributions of suspended clay minerals to the aggregation and subsequent preservation of filamentous photosynthetic cyanobacteria. The electrostatic attraction between the oppositely charged surfaces of cyanobacteria and clay minerals is the main driving force of cyanobacteria-clay co-aggregation. The deprotonation of —COOH groups on cyanobacteria and therefore the release of H^+ result in local dissolution of Si from the clay minerals. The influence of the abundances of dissolved ions on the aggregation of cyanobacteria is a relatively minor factor compared to that of clay minerals, although the presence of ions is capable of enhancing the formation of cyanobacteria-clay co-aggregates. Clay-cyanobacteria co-aggregation generally occurs at low concentrations of suspended clay particles, regardless of the types of suspended clay minerals, indicating that co-aggregation happens readily and likely facilitates the preservation of cyanobacteria in a wide variety of shallow marine environments. Consequently, suspended detrital clay minerals should be considered as a key factor for understanding the microbial preservation in shallow marine environments, and its potential impact on marine elemental cycles through the dissolution of clay minerals also warrants further investigation.

Declaration of Competing Interest

No conflict of interest exists in the submission of this manuscript, and the manuscript is approved by all authors for publication. I would like to declare on behalf of my co-authors that the work described was original research that has not been published previously, and not under consideration for publication elsewhere, in whole or in part. All the authors listed have approved the manuscript that is enclosed.

Acknowledgments

This work was supported by National Special Support for High-Level Personnel, National Natural Science Foundation of China (Grant No. 41772041 and 41802038), Youth Innovation Promotion Association CAS for the excellent member (2016-81-01) and National Postdoctoral Program for Innovative Talents (Grant No. BX201600165). This is a contribution No. IS3020 from GIGCAS.

Appendix A. Supplementary data

Supplementary data to this article can be found online at https://doi.org/10.1016/j.chemgeo.2021.120285.

References

Anderson, R.P., Tosca, N.J., Gaines, R.R., Mongiardino Koch, N., Briggs, D.E.G., 2018. A mineralogical signature for Burgess Shale–type fossilization. Geology 46, 347–350.
Anderson, R.P., Tosca, N.J., Cinque, G., Frogley, M.D., Lekkas, I., Akey, A., Hughes, G.M., Bergmann, K.D., Knoll, A.H., Briggs, D.E.G., 2020a. Aluminosilicate haloes preserve complex life approximately 800 million years ago. Interface Focus 10, 20200011.
Anderson, R.P., Tosca, N.J., Saupe, E.E., Wade, J., Briggs, D.E.G., 2020b. Early formation and taphonomic significance of kaolinite associated with Burgess Shale fossils. Geology. https://doi.org/10.1130/G48067.1 (in press).
Bartley, J.K., 1996. Actualistic taphonomy of Cyanobacteria: implications for the Precambrian fossil record. Palaios 11, 571–586.
Betts, H.C., Puttick, M.N., Clark, J.W., Williams, T.A., Donoghue, P.C.J., Pisani, D., 2018. Integrated genomic and fossil evidence illuminates life's early evolution and eukaryote origin. Nat. Ecol. Evol. 2, 1556–1562.
Brasier, M.D., Wacey, D., Mcloughlin, N., 2011. Taphonomy in temporally unique settings: an environmental traverse in search of the earliest life on Earth. In: Allison, P.A., Bottjer, D.J. (Eds.), Taphonomy. Springer, Netherlands, pp. 487–518.
Brasier, M.D., Antcliffe, J., Saunders, M., Wacey, D., 2015. Changing the picture of Earth's earliest fossils (3.5-1.9 Ga) with new approaches and new discoveries. Proc. Natl. Acad. Sci. U. S. A 112, 4859–4864.
Brigatti, M.F., Galan, E., Theng, B.K.G., 2013. Structures and mineralogy of clay minerals. In: Bergaya, F., Lagaly, G. (Eds.), Developments in Clay Science. Elsevier, Amsterdam, pp. 19–86.
Butterfield, N.J., 1990. Organic preservation of non-mineralizing organisms and the taphonomy of the Burgess Shale. Paleobiology 16, 272–286.
Butterfield, N.J., 1995. Secular distribution of Burgess-Shale-type preservation. Lethaia 28, 1–13.
Cuadros, J., Afsin, B., Jadubansa, P., Ardakani, M., Ascaso, C., Wierzchos, J., 2013. Microbial and inorganic control on the composition of clay from volcanic glass alteration experiments. Am. Mineral. 98, 319–334.
Dere, S., Güneş, T., Sivaci, R., 1998. Spectrophotometric determination of chlorophyll – a, b and total carotenoid contents of some algae species using different solvents. Botany 22, 13–17.
Dittrich, M., Sibler, S., 2005. Cell surface groups of two picocyanobacteria strains studied by zeta potential investigations, potentiometric titration, and infrared spectroscopy. J. Colloid Interface Sci. 286, 487–495.
Djomgoue, P., Njopwouo, D., 2013. FT-IR spectroscopy applied for surface clays characterization. J. Surface Eng. Mater. Adv. Technol. 3, 275–282.
Emmerich, K., 2013. Full characterization of smectites. In: Bergaya, F., Lagaly, G. (Eds.), Developments in Clay Science. Elsevier, Amsterdam, pp. 381–404.
Fein, J.B., Duaghney, C.J., Yee, N., Davis, T.A., 1997. A chemical equilibrium model for metal adsorption onto bacterial surfaces. Geochim. Cosmochim. Acta 61, 3319–3328.
Fein, J.B., Scott, S., Rivera, N., 2002. The effect of Fe on Si adsorption by *Bacillus subtilis* cell walls: insights into non-metabolic bacterial precipitation of silicate minerals. Chem. Geol. 182, 265–273.
Ferris, F.G., Fyfe, W.S., Beveridge, T.J., 1988. Metallic ion binding by *Bacillus subtilis*: Implications for the fossilization of microorganisms. Geology 16, 149–152.
Gaines, R.R., 2014. Burgess Shale-type preservation and its distribution in space and time. Paleontol. Soc. Pap. 20, 123–146.
Gauger, T., Byrne, J.M., Konhauser, K.O., Obst, M., Crowe, S., 2016. Influence of organics and silica on Fe(II) oxidation rates and cell-mineral aggregate formation by the green-sulfur Fe(II)-oxidizing bacterium *Chlorobium ferrooxidans* KoFox – Implications for Fe(II) oxidation in ancient oceans. Earth Planet. Sci. Lett. 443, 81–89.
Gehlen, M., Beck, L., Calas, G., Flank, A.M., Benneckom, A.J.V., Beusekom, J.E.E.V., 2002. Unraveling the atomic structure of biogenic silica: evidence of the structural association of Al and Si in diatom frustules. Geochim. Cosmochim. Acta 66, 1601–1609.
Goldberg, E.D., Arrhenius, G.O.S., 1958. Chemistry of Pacific pelagic sediment. Geochim. Cosmochim. Acta 13, 153–198.
Haghighi, O., Shahryari, S., Ebadi, M., Modiri, S., Zahiri, H.S., Maleki, H., Nghabi, K.A., 2017. *Limnothrix* sp. KO05: a newly characterized cyanobacterial biosorbent for cadmium removal: the enzymatic and non-enzymatic antioxidant reactions to cadmium toxicity. Environ. Toxicol. Pharmacol. 51, 142–155.
Hazen, R.M., Sverjensky, D.A., Azzolini, D., Bish, D.L., Elmore, S.C., Hinnov, L., Milliken, R.E., 2013. Clay mineral evolution. Am. Mineral. 98, 2007–2029.
Hu, X., Wang, Y.L., Schmitt, R.A., 1998. Geochemistry of sediments on the Rio Grande Rise and the redox evolution of the South Atlantic Ocean. Geochim. Cosmochim. Acta 52, 201–207.
Jeandel, C., Oelkers, E.H., 2015. The influence of terrigenous particulate material dissolution on ocean chemistry and global element cycles. Chem. Geol. 395, 50–66.
Jones, C., Nomosatryo, S., Crowe, S.A., Bjerrum, C.J., Canfield, D.E., 2015. Iron oxides, divalent cations, silica, and the early earth phosphorus crisis. Geology 43, 51–68.
Konhauser, K.O., Fyfe, W.S., Ferris, F.G., Beveridge, T.J., 1993. Metal sorption and mineral precipitation by bacteria in two Amazonian river systems: Rio Solimões and Rio Negro, Brazil. Geology 21, 1103–1106.
Lagaly, G., Dékány, I., 2013. Colloid clay science. In: Bergaya, F., Lagaly, G. (Eds.), Developments in Clay Science. Elsevier, Amsterdam, pp. 243–345.
Li, J., Benzerara, K., Bernard, S., Beyssac, O., 2013. The link between biomineralization and fossilization of bacteria: insights from field and experimental studies. Chem. Geol. 359, 49–69.
Liu, D., Yuan, P., Liu, H., Li, T., Tan, D., Yuan, W., He, H., 2013. High-pressure adsorption of methane on montmorillonite, kaolinite and illite. Appl. Clay Sci. 85, 25–30.
Ma, K., 1997. Effect of interaction between clay particles and Fe^{3+} ions on colloidal properties of kaolinite suspensions. Clay Clay Miner. 45, 733–744.
Madejová, J., 2001. Baseline studies of the clay minerals society source clays: infrared methods. Clay Clay Miner. 49, 372–373.
Madejová, J., Bujdák, M., Janek, M., Komadel, P., 1998. Comparative FT-IR study of structural modifications during acid treatment of dioctahedral smectites and hectorite. Spectrochim Acta A 54, 1397–1406.
Martinez, R.E., Pokrovsky, O.S., Schott, J., Oelkers, E.H., 2008. Surface charge and zeta-potential of metabolically active and dead cyanobacteria. J. Colloid Interface Sci. 323, 317–325.
McMahon, S., Anderson, R.P., Saupe, E.E., Briggs, D.E.G., 2016. Experimental evidence that clay inhibits bacterial decomposers: implications for preservation of organic fossils. Geology 44, 867–870.
Milliman, J.D., Fan, L., Zhao, Y., Zheng, T., Limeburner, R., 1996. Suspended matter regime in the Yellow Sea. Prog. Oceanogr. 17, 215–227.
Newman, S.A., Mariotti, G., Pruss, S., Bosak, T., 2016. Insights into cyanobacterial fossilization in Ediacaran siliciclastic environments. Geology 44, 579–582.
Newman, S.A., Klepac-Ceraj, V., Maritti, G., Pruss, S.B., Watson, N., Bosak, T., 2017. Experimental fossilization of mat-forming cyanobacteria in coarse-grained siliciclastic sediments. Geobiology 15, 484–498.
Orr, P.J., Briggs, D.E.G., Kearns, S.L., 1998. Cambrian Burgess Shale animals replicated in clay minerals. Science 281, 1173–1175.
Petrovich, R., 2001. Mechanisms of fossilization of the soft-bodied and lightly armored faunas of the Burgess Shale and of some other classical localities. Am. J. Sci. 301, 683–726.
Playter, T., Konhauser, K., Owttrim, G., Hodgson, C., Warchola, T., Mloszewska, A.M., Sutherland, B., Bekker, A., Zonneveld, J.P., Pemberton, S.G., Gingras, M., 2017.

Microbe-clay interactions as a mechanism for the preservation of organic matter and trace metal biosignatures in black shales. Chem. Geol. 459, 75–90.
Saito, M., 2016. Hydrosphere as microbial habitat. In: Ehrlich, H.L., Newman, D.K., Kappler, A. (Eds.), Geomicrobiology, Six ed. CRC Press, New York, pp. 97–128.
Sánchez-Baracaldo, P., 2015. Origin of marine planktonic cyanobacteria. Sci. Rep. 5, 17418. https://doi.org/10.1038/srep17418.
Sánchez-Baracaldo, P., Cardona, T., 2020. On the origin of oxygenic photosynthesis and Cyanobacteria. New Phytol. 225, 1440–1446.
Santschi, P.H., Balnois, R., Wilkinson, K.J., Zhang, J., Buffle, J., Guo, L.D., 1998. Fibrillar polysaccharides in marine macromolecular organic matter as imaged by atomic force microscopy and transmission electron microscopy. Limnol. Oceanogr. 43, 896–908.
Sinetova, M.A., Červený, J., Zavřel, T., Nedbal, L., 2012. On the dynamics and constraints of batch culture growth of the cyanobacterium *Cyanothece* sp. ATCC 51142. J. Biotechnol. 162, 148–155.
Tang, T.T., Kisslinger, K., Lee, G., 2014. Silicate deposition during decomposition of cyanobacteria may promote export of picophytoplankton to the deep ocean. Nat. Commun. 5, 4143. https://doi.org/10.1038/ncomms5143.
Tarhan, L.G., Hood, A.V.S., Droser, M.L., Gehling, J.G., Briggs, D.E.G., 2016. Exceptional preservation of soft-bodied Ediacara Biota promoted by silica-rich oceans. Geology 44, 951–954.
Tosca, N.J., Johnston, D.T., Mushegian, A., Rothman, D.H., Summons, R.E., Knoll, A.H., 2010. Clay mineralogy, organic carbon burial, and redox evolution in Proterozoic oceans. Geochim. Cosmochim. Acta 74, 1579–1592.
Tournassat, C., Ferrage, E., Poinsignon, C., Charlet, L., 2004. The titration of clay minerals II. Structure-based model and implications for clay reactivity. J. Colloid Interface Sci. 273, 234–246.
Wacey, D., Saunders, M., Roberts, M., Menon, S., Green, L., Kong, C., Culwick, T., Strother, P., Brasier, M.D., 2014. Enhanced cellular preservation by clay minerals in 1 billion-year-old lakes. Sci. Rep. 4, 5841.
Wightman, P.G., Fein, J.B., 2005. Iron adsorption by Bacillus subtilis bacterial cell walls. Chem. Geol. 216, 177–189.
Yee, N., Phoenix, V.R., Konhauser, K.O., Benning, L.G., Ferris, F.G., 2003. The effect of cyanobacteria on silica precipitation at neutral pH: implications for bacterial silicification in geothermal hot springs. Chem. Geol. 199, 83–90.
Yee, N., Benning, L.G., Phoenix, V.R., Ferris, F.G., 2004. Characterization of metal-cyanobacteria sorption reactions: a combined macroscopic and infrared spectroscopic investigation. Environ. Sci. Technol. 38, 775–782.